Affordable GNSS PPP Results as Constraints for Pressure Time Series Offshore

Johnson OGUNTUASE, Uchenna NWANKWO, Stephan HOWDEN, USA

Keywords: affordable GNSS, GNSS buoy, PPP, RTK, Vdatum, water level, GNSS buoy

SUMMARY

This paper discusses offshore water level measurements and the accuracies possible using affordable GNSS receivers (<$2000). The goal is to develop an affordable and straightforward technique capable of continuous and accurate water level measurements at remote locations towards addressing the uncertainties inherent in the tidal datum transformation model offered by NOAA's Vdatum. This technique can be used either directly for tidal datum transfer when 30 plus days of GNSS data acquisition is possible or in short-term simultaneous observations with a seafloor-mounted pressure gauge to reference the longer term (30+ days) pressure time series to the ellipsoid before tidal datum transfer is performed. We applied precise point positioning (PPP) results from an affordable GNSS receiver to constrain pressure sensor measurements to the ellipsoid. Limiting Vdatum uncertainties below 10 cm at a 95 % confidence level would require that GNSS height uncertainties be less than 5 cm in the error budget. It is then desirable to investigate the order of PPP vertical positioning accuracies possible with such a receiver on a dynamic platform at sea. We conducted two experiments at different locations offshore using GNSS+INS sensors to validate the affordable PPP vertical positioning results. The GNSS+INS sensors in the post-processed kinematic (PPK) strategy validate the affordable PPP vertical position results. We note that the second experiment's results are more consistent than the first following accurate lever-arms measurements for the GNSS antennas installed on an Echo boat (small uncrewed surface vehicle). Comparing water level moving averages between the two processing strategies shows a mean difference of 4 cm. That result compares instantaneous GNSS heights from the affordable receiver without accounting for induced heave, suggesting that attitude measurements at sea for short lever arms are negligible. Briefly discussed is the preliminary validation of the tidal datum determination offshore using the affordable vertical positions as the constraint.

Affordable GNSS PPP Results as Constraints for Pressure Time Series Offshore

Johnson OGUNTUASE, Uchenna NWANKWO, Stephan HOWDEN, USA

1. INTRODUCTION

This study aims to show the utility of affordable GNSS receivers on a floating platform, such as a buoy or Autonomous Surface Vessel, in a newly developed approach to vertically reference seafloor pressure measurements of water level to a geodetic reference system. This would allow a seafloor pressure record to be used in a tidal datum transfer exercise to obtain tidal datums to the ellipsoid and used to validate and improve tools such as NOAA's VDatum (Parker et al., 2003) that, for example, allow hydrographic surveys to be referenced relative to the ellipsoid, eliminating complications of heave and tidal measurements, and then converted to chart datum (Mean Lower Low Water in the U.S.).

The GNSS market has seen rapid developments in GNSS hardware and allied sensors required for autonomous driving technology implementation driven by investments in the autonomous car industry. Hence the proliferation of different GNSS hardware grades ranging from smartphone chipsets to low-cost/mass markets development kits capable of tracking single- or multi-constellations and single- or multi-frequencies. The rapid proliferation of GNSS hardware enables various location-based applications, consequently driving studies on affordable/mass-market GNSS hardware. Many studies (Aggrey et al., 2019; Banville et al., 2019; Gill et al., 2018; Nie et al., 2020; Oguntuase, 2020) exist on GNSS hardware characteristics and performances in different positioning and navigation strategies. The mass market literature describes some non-geodetic GNSS receivers (capable of combining single- or multi-frequency and single- or multi-GNSS) as low-cost, mass-market, cost-effective, or affordable. That classification stems from their tracking quality, prices (tens of dollars to a few hundred), and overall product features.

Some FIG publications address related studies (Arnell et al., n.d.; Lipatnikov & Shevchuk, 2019; Weston & Dr. Volker Schwieger, 2010). However, studies on low-cost/affordable GNSS receivers for precise point positioning (PPP) at offshore locations are scarce. In this work, we demonstrate the potential of an affordable GNSS receiver (<$2000) in addressing the uncertainties inherent in the tidal datum extension offshore. For instance, Nwankwo et al., 2020 discuss errors in NOAA's Vdatum model (Parker et al., 2003) for seamless transformations between different height systems in the United States.

The first reduction tidal datums are average levels, ranges, or tide phases, computed over the lunar nodal cycle (~19 years). Many water level gauges have not been in operation for 19 years, and so methods have been developed to use simultaneous measurements from a short-term (subordinate) gauge and a long-term control (primary) gauge, and the 19-year datums from the control gauge, to estimate equivalent 19-year datums for the subordinate gauge (Gill

and Schultz, 2001). Swanson (1974) estimated the uncertainties in tidal datums from tidal datum transfers for varying lengths of simultaneous subordinate and primary water level records and obtained values of 0.040 m for a 1-month simultaneous record on the east and west coasts and 0.055 m on the coast of the Gulf of Mexico. In the context of the allowed Total Vertical Uncertainty allowed for an Order 1a hydrographic survey in 20 m of water of 0.564 m or Special Order of 0.292 m (IHO, 2020), these uncertainties are 7% and 14% for Order 1a and Special Order, respectively on the west and east coasts and 14% and 19%, respectively on the Gulf Coast.

Information on geodetically referenced offshore tidal datums can be obtained using GNSS buoys (e.g., Hocker and Wardell, 2010; Nwankwo et al., 2020). However, on the coastal water of the northern Gulf of Mexico, the authors have not been successful in keeping a moored GNSS buoy out for more than a couple of weeks without it being vandalized, as reported in Nwankwo et al., 2020. Utilizing the hydrostatic equation, information on the density of the water column, and sea level barometric pressure, a seafloor-mounted pressure gauge can measure the water levels above it, but there is no absolute reference for the measurements. However, a short-term (>= 6 hours) simultaneous geodetically measured sea level from a buoy or ASV and a pressure gauge can be used to reference, geodetically, the water levels from the pressure gauge. The resulting water level can then be used in a tidal datum transfer.

In this work, we describe the concept where a 30-day GNSS observation is unavailable but uses 6-hour PPP results (or more) as constraints for pressure measurements (> 30 days). Next, we evaluate the PPP results using the affordable GNSS receiver aboard an uncrewed surface vehicle (USV) at an offshore location relative to post-processed kinematic (PPK) results from co-located GNSS+INS hardware. Though GNSS buoy for tidal datum determination is not new (André et al., 2013; Bisnath et al., 2003; Cheng et al., 2004; Dodd, 2009; Hocker & Wardwell, 2010; Knight et al., 2020; Lin et al., 2017), evaluating the PPP results from the affordable GNSS receiver becomes essential as we note that such studies are scarce. This paper presents the preliminary results of 30-day water level observations using the PPP results as constraints for pressure measurement. However, we limit our discussions to concept descriptions and PPP accuracies at offshore locations. Since it is logical to separate oceanographic computations from GNSS computations, we will discuss the seafloor data, the analysis, and tidal datum transfer in a follow-up paper.

2. EXPERIMENT DESIGN

Figure 1 presents the overview of the experiment design, providing a roadmap to reproducing our results. The procedure is as follows:

1. Collect co-located GNSS and pressure measurements at an offshore location
2. Validate PPP-derived water level from an affordable GNSS receiver, using results from a geodetic grade GNSS+INS sensor in the PPK strategy
3. Validate seafloor pressure data.
4. Constrain the seafloor data to a reference ellipsoid (e.g., WGS84 or NAD83 ellipsoid)
5. Prepare preliminary water levels from the seafloor data
6. Compute and validate tidal datums and water levels

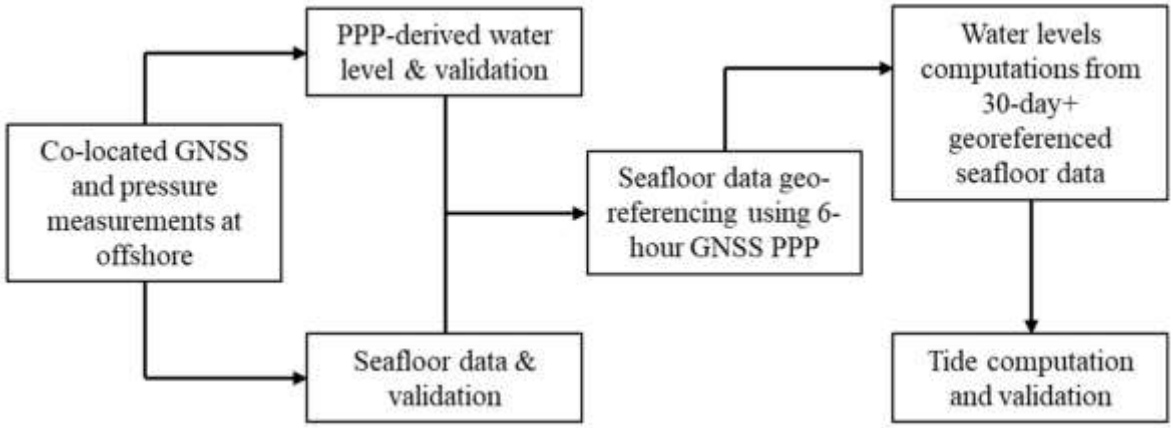

Figure 1 Experiment design flowchart.

As we mentioned in the introduction, details about seafloor data validation and datum computations will come in a follow-up paper. We demonstrate the repeatability of our results using the GNSS PPP and pressure measurement approach for determining water levels by acquiring data in two experimental setups that utilized an affordable GNSS receiver, RBR Concerto CTD, RBR Digiquartz pressure sensor, and a Teledyne/RDI ADCP (all oceanographic sensors housed in one single underwater package), in separate deployments. **Table 1** lists the sensors and the manufacturer's name. It bears repeating that the GNSS+INS sensor is only required to verify the affordable GNSS PPP results offshore.

Table 1 GNSS and presseure sensor hardware

Hardware	Description
Applanix POS-MV	GNSS+INS
Septentrio Mosaic	GNSS receiver
RBRconcerto	CTD
RBRquartzQ	Paroscientific DigiQuartz pressure sensor 55 dbar
ADCP	Teledyne/RDI

2.1 Experiment Locations

The first experiment occurred on May 27, 2021, at 29.9858N, 088.5379W (**Figure 2**). We deployed a USV (EchoBoat) housing a Septentrio Mosaic GNSS receiver and a survey-grade GNSS+INS from one of the University of Southern Mississippi's (USM) research vehicles, R/V Point Sur. The second experiment occurred at 26.61589N, 88.41786W on March 1, 2022, using the same GNSS receiver and tactical-grade GNSS+INS hardware aboard a different USV (SeaTrac).

Figure 2 Left panel: EchoBoat deployment. Center panel: experiment #1 and #2 locations: 52.4 and 78.6 km from the nearest CORS (ALDI). PCLA, DSTN, and PNMA (are towards the east but not shown); they enclosed location #2 in the CORS network. Right panel: Bottom package deployment.

2.2 Operational Concept

GNSS-derived water level measurement technique is well-known (André et al., 2013; Bisnath et al., 2003; Cheng et al., 2004; Dodd, 2009; Hocker & Wardwell, 2010; Knight et al., 2020; Lin et al., 2017) and has been proposed for water level observations, tidal datum extensions, and datum improvements (Bisnath et al., 2003; Cheng et al., 2004; Dodd, 2009; Hocker & Wardwell, 2010). However, utilizing the technique for tidal datum extension offshore would require at least 30-day GNSS water level observations to estimate the tidal signal constituents. Furthermore, such observation aboard a buoy or a USV may utilize quality and cost-effective sensors like the affordable GNSS receiver.

The new concept requires sea surface deployment of a GNSS buoy or a USV with GNSS onboard and a seafloor deployment of a pressure sensor. The GNSS buoy, or USV with GNSS, need only be moored or kept on the station long enough to compute the separation (H + O + D) value to the desired accuracy, where H, O, and D are the ellipsoidal height, O is the GNSS antenna offset above the sea surface, and D is the water depth from the sea surface. It can then be removed to avoid vandalization, and the bottom mooring can collect offshore water level records for 30 days or more for tidal datum determination. One advantage of using the USV's station-keeping command is the ease of maintaining the exact location as the

deployed bottom package in autopilot mode. That feature allows the vessel intermittently return to the preset location once it drifts out of the redefined radius. In addition, the bottom package is equipped with mooring flotation devices, which allows using acoustic releases for retrieval. That concepts also preclude the bottom package vandalization.
Figure 3 describes the operational concept where the water depth D is computed from the hydrostatic equation using the bottom, surface temperature, and salinity values for density computation. The offset from the USV to the water line is measured as O, and PPP processing is used to measure the GNSS antenna height from WGS84 and transformed to NAD83 ellipsoid.

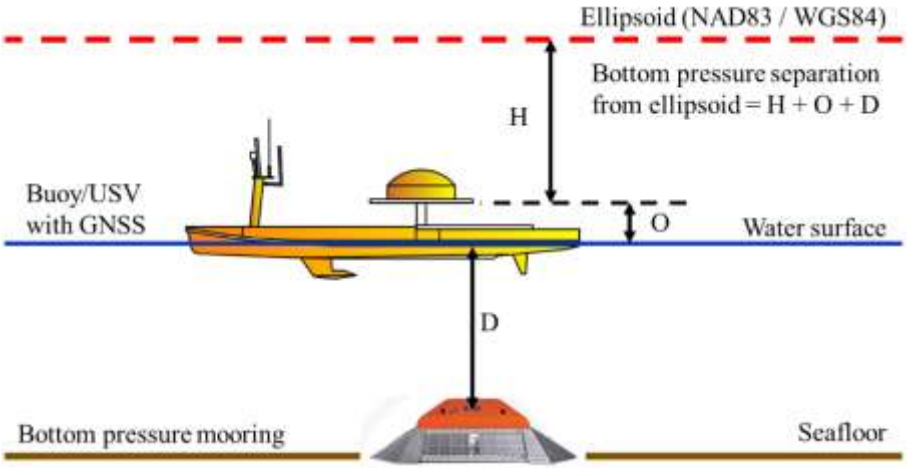

Figure 3 The operational concept uses a GNSS receiver installed on either a buoy or a USV and a bottom package containing a pressure sensor to estimate seafloor separation from the ellipsoid.

3. PROCESSING STRATEGY

Since numerous publications exist on GNSS processing strategies and algorithms, we omit that discussion here due to page limit restrictions. Hence the focus on concepts and the results. We used JPL's GipsyX and Hexagon-Novetel GrafNav PPP processing engines for the PPP data processing for the data acquired with the affordable GNSS receiver. For the GNSS+INS dataset, we used the Applanix POSPAC MMS's Smartbase processing engine. The PPP processing accounted for Earth deformations (ocean loading, Earth tide, and pole tides). However, validating the offshore PPP results is not straightforward, as the reference solutions, in other words, the survey-grade GNSS+INS navigation solutions required for the comparison, posed some challenges.

Such a challenge is typical whenever remote locations are outside the CORS network, precluding accurate correction estimates for the virtual reference station in the virtual reference station (VRS) or network PPK strategy. Since ionospheric-free combinations efficiently mitigate that error, the major challenge is the wet and dry tropospheric delays, which deteriorate as distances increase from reference stations. In addressing that challenge, we ensured the GNSS+INS dataset enclosure within the CORS network for high-quality PPK

results needed to validate the PPP. All the GNSS processing used the products from the Center for Orbit Determination in Europe (CODE).

All processing accounted for lever arms measurements, GNSS antenna phase center, and offsets corrections to reduce GNSS ellipsoidal heights to the sea surface. The first experiment used measuring tape to determine the offsets, while the second used the total station technique. Though it should be intuitive why precise lever arm determination is essential, the results in the second experiment and the subsequent summary emphasize that regardless of whether the vessels involved are small or large. Additionally, following previous discussions on tilt measurements to water level (Dodd, 2009; Hocker & Wardwell, 2010; Lin et al., 2017), we investigate whether tilt measurements in accounting for induced heave play a significant role when the antenna lever arm less than a meter, as in both experiments.

4. RESULTS

One of the goals of this work is to justify using affordable GNSS receivers with reasonable quality for high-accuracy kinematic PPP in GNSS water level determination. Hence, we briefly examine the phase residuals in different ionospheric-free combinations for different constellations; we describe the PPP results (from affordable GNSS receiver) and their validation relative to the PPK results (from survey-grade GNSS+INS); we present the validation summary statistics and the presents the pressure measurement results.

4.1 GNSS Data Quality Issues

Figure 4 (left panel) shows the number of satellites (SVs) used in GipsyX PPP solutions for data acquired at Experiment location #1, and **Figure 4** (right panel) shows the phase residuals. Over the seven-hour observation period, the number of GPS (G) SVs used for the PPP solution is consistently higher than others. GPS contribution to the multi-GNSS PPP solution ranges between seven and twelve SVs, while BeiDou (C) and GLONASS (R) contributions are between four and nine. The effects of those contributions appear in the phase residuals in the panel to the right, revealing GPS with the best phase residuals – the 95% statistic is 2.6 cm. The histograms show narrow distributions for GPS, GLONASS, and Galileo, whereas BeiDou's distribution is wide. Consequently, the GPS, GLONASS, and Galileo's contribution to PPP solutions offshore should yield more reliable results without the BeiDou system when using CODE products.

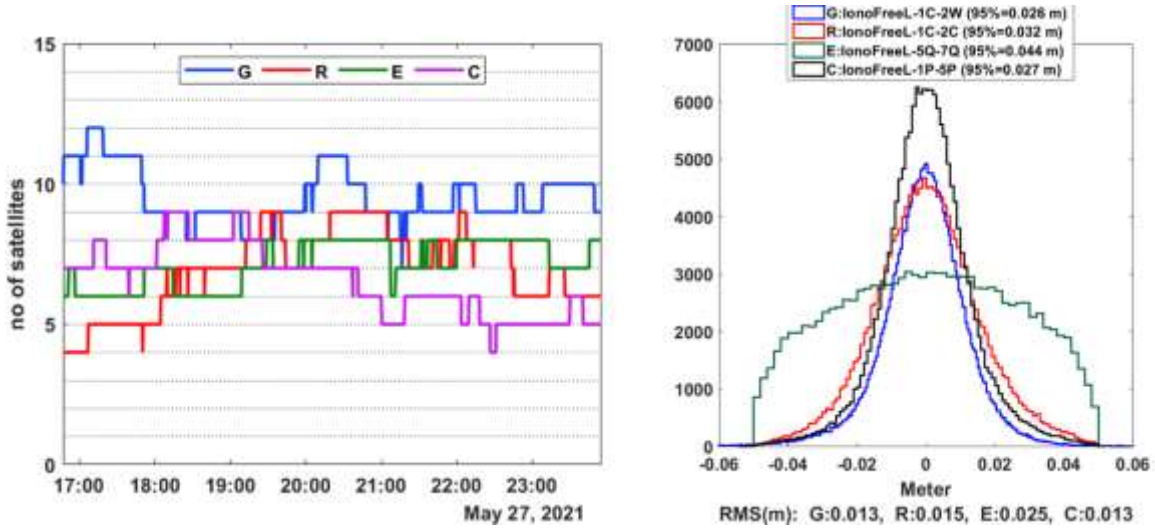

Figure 4: Left panel: number of satellites included in GipsyX PPP solution at Experiment location #1. Right panel: carrier phase residual distribution and the corresponding RMS values.

4.2 PPP Results

Figure 5 and **Figure 6** (left panels) present the PPP-derived water level time series (1 Hz) for 7- and 8-hour observations from the affordable GNSS receiver. The right panels in those figures show the PPK-derived water level time series (50 Hz) from the GNSS+INS hardware. A 3-minute low-pass filter (LPF) cutoff (3-minute moving average) is applied to all datasets to remove high-frequency signals such as the surface gravity waves. The blue and red lines in the figures represent the filtered water levels from the PPP (GNSS-only) and PPK (GNSS+INS) results, respectively.

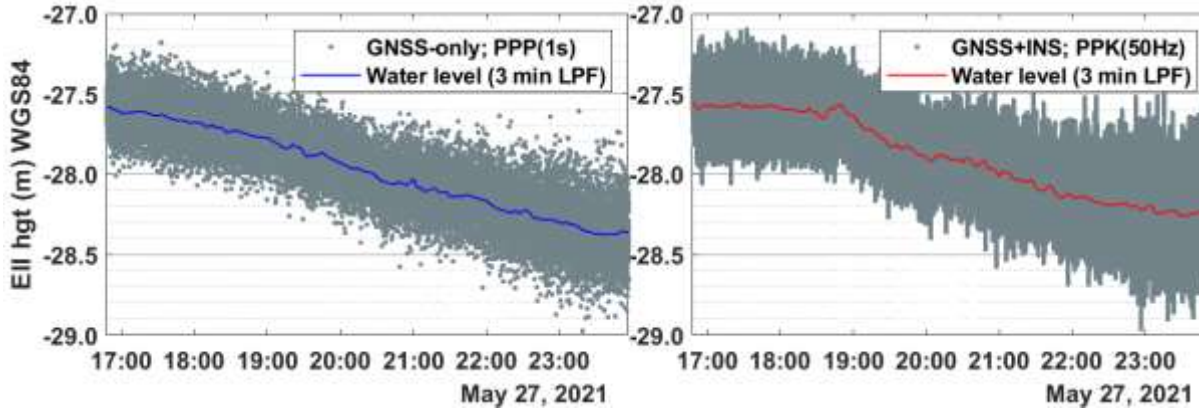

Figure 4 Instantaneous water levels (gray dots) at experiment location #1. Left panel: PPP results (1 Hz) from affordable GNSS. Right panel: PPK results from survey-grade GNSS+INS (50 Hz). The blue and red lines are the water levels using the 3-minute LPF cutoff.

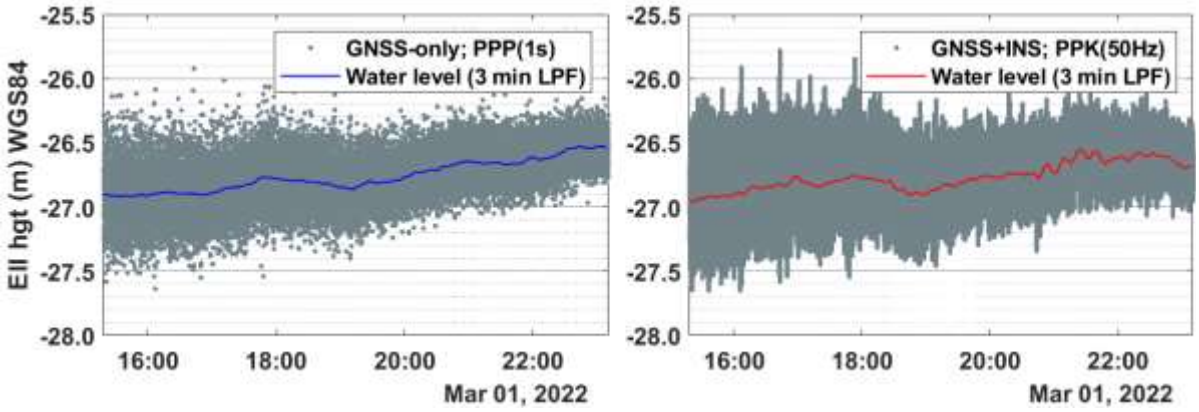

Figure 6 Instantaneous water levels (gray dots) at experiment location #2. The graphics description is the same as described in **Figure 5**.

4.3 Kinematic PPP Validation

Figure 7 and Figure 8 summarize the averaged water level results. The serial difference in water levels derived from the two hardware and processing strategies offers an insight into the PPP quality obtainable with a mass market GNSS receiver on a dynamic offshore platform. The histograms in the left panels of those figures describe the PPP versus PPK differences. Table 2 summarises the statistics. The 95% ordered statistic for the water level differences at location #1 and location #2 are 14 and 11 cm, respectively. The means are 7.9 and 0.5 cm, while the standard deviations (1 sigma) are 3.9 and 5.4 cm, respectively. The difference histogram at location #1 (**Figure 7**) shows a bias between the PPP and PPK solutions. We attribute that to the lever arm measurement quality. In contrast with the histogram at location 2 (**Figure 8**), the bias is near zero (5 mm). Again that emphasizes the need for precise lever arm measurements with a total station or any other precise measurement method irrespective of the vessel size.

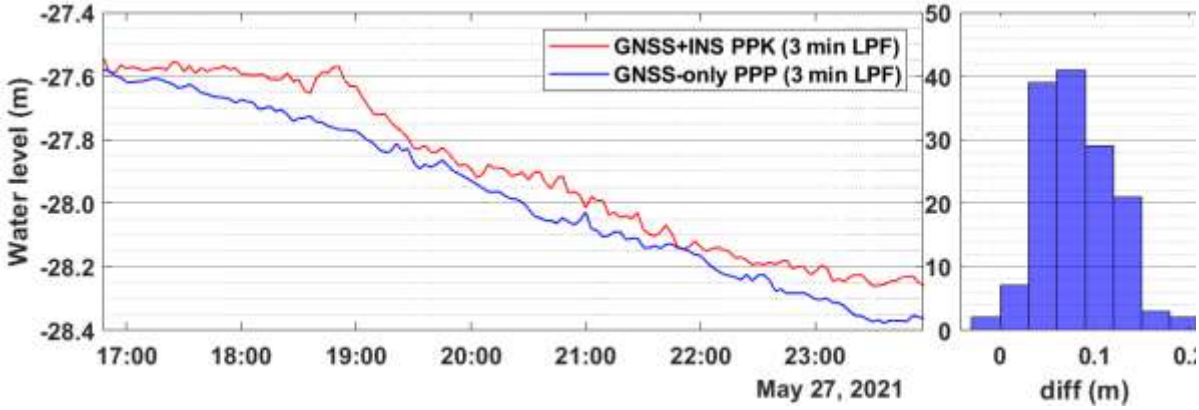

Figure 7 Left panel: averaged water levels from GNSS-only and GNSS PPK results aboard EchoBoat (USV) location #2. Right panel: averaged water level difference.

Designating the PPK results as the reference solution, assuming it has better positioning quality than the PPP results, the statistics suggest the worst PPP positioning quality is 14 cm relative to the PPK. Though typical uncertainties for PPK-derived vertical position is about 5

cm, vertical uncertainties for kinematic PPP are slightly higher. Notably, a 10-cm difference in kinematic PPP vertical positions is not entirely outside typical kinematic PPP results using the traditional PPP algorithm, which does not explicitly account for instrument code- and phase biases, resulting in a non-integer ambiguity resolution. However, an improvement in that vertical positioning accuracy with the receiver is possible by eliminating data with non-gaussian distributing from contribution to the PPP solution.

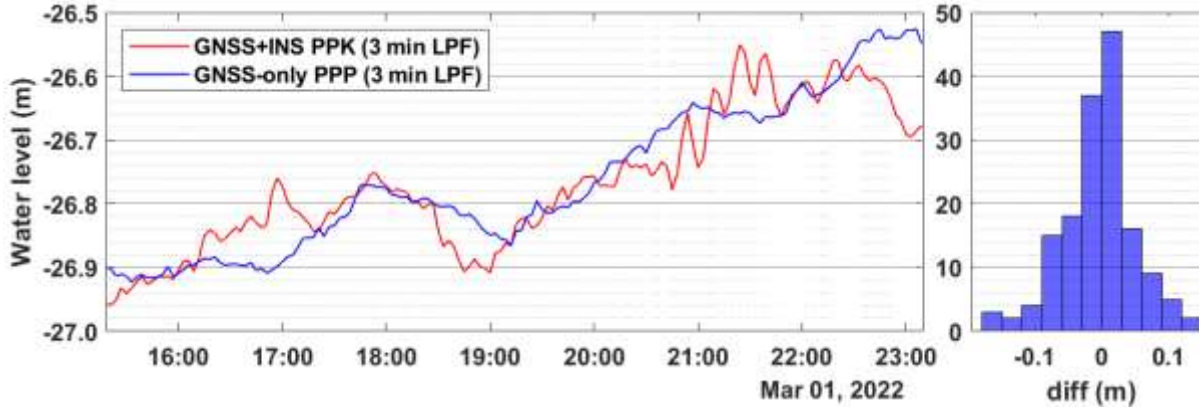

Figure 8 Left panel: averaged water levels from GNSS-only and GNSS PPK results aboard SeaTrac (USV) at location #2. Right panel: averaged water level difference.

Intuitively, one may suspect the induced-heave effect on the PPP-derived water level averages since the PPP processing does not account for the roll and pitch effects in the GNSS-only observations. However, we quantified that effect by applying the roll and pitch results from the GNSS+INS hardware to the affordable GNSS receiver's lever arm using **Equation 1**.

$$\boldsymbol{H_{induced} = -x\,sin\,(P) - y\,sin\,(R)\,cos\,(P) + z\left(1 - cos\,(R) cos\,(P)\right)}, \qquad (1)$$

Vector [x, y, z] is the antenna lever arms from the vessel's / platform's reference origin, with x pointing towards the bow in a right-handed system, y pointing to the port, and z pointing in the up direction, P and R are the roll and pitch angles (Hare et al., 1995). The antenna lever arms on both vessels in the two experiments, ordered as [x, y, z], are $[1.371, 0.015, 0.343]_m$ and $[-0.396, 0.007, 0.4650]_m$. The roll and pitch enviroments for the experiment locations are listed in **Table 2**. Those values indicate the vessel's attitude at sea, which explains why the PPP results match the reference solutions (GNSS+INS) in the experiment at location #1 compared to the results in location #2. Another reason for the better roll-pitch environment at location two is that the platform (SeaTrac) is larger than the Echo-Boat. Also, SeaTrac operated in autopilot mode, unlike the Echo-Boat, which lost its navigation and autopilot functionality at sea, thus requiring mooring at the observation station.

Table 2 Roll and pitch statistics (1 Hz) and the maximum absolute induced heaves

	Roll (degree)		Pitch (degree)		Induced heave (m)	
	min	max	min	max	max (1-sec)	max (LPF)
Experiment #1	–22.909	24.447	–19.454	15.936	0.133	0.007
Experiment #2	–24.790	24.604	–13.131	11.432	0.298	0.006

Passing the instantaneous PPP results for experiment 1 with the induced-heave corrections applied through the 3-minute LPF shows that the resulting water levels have a near-zero difference (1 cm) for most epochs (75^{th} percentile) compared to the statistics for water levels from GNSS-only PPP results without induced-heave corrections. However, LPF reduces the induced heave from ± 13 cm in extreme cases (outside 0.01 and 99.99 percentile bounds) to near zero (± 0.3 cm). That agrees somewhat with Dodd, 2009's comment about the induced heave effect reducing drastically to ~ 2 cm from 10 cm in a 6-minute LPF cutoff. The induced heave effects and characteristics in experiment 2 results are similar to those described afore

Table 3 summarizes the statistics comparing PPP results with and without induced heave applied relative to the GNSS+INS solutions. Comparing the 95% ordered statistics in the third and sixth columns reveals that the induced heave effect is less than 1 cm for a short lever arm.

Table 3 Low-pass filtered water levels statistics from PPP versus PPK results

	GNSS-only PPP versus GNSS+INS PPK			GNSS-only PPP (induced heave applied) versus GNSS+INS PPK		
	mean	1-sigma	95%	mean	std	95%
Experiment #1	0.079	0.039	0.141	0.079	0.039	0.142
Experiment #2	–0.005	0.054	0.120	–0.010	0.054	0.114

4.4 Preliminary water levels

We present the preliminary water level (> 30 days), demonstrating the concept here. The 1 Hz GNSS solutions were averaged over 3-minute intervals to mitigate the contributions of surface gravity waves to the sea surface. Over the simultaneous observation period (T_s> 6 hrs), the mean sea level to the ellipsoid from the PPP solutions was added to the mean sea level from the pressure record to reference the pressure record to the ellipsoid. For this paper, the important uncertainty to quantify is the mean sea level from the PPP solutions. During T_s, there was a decrease in the tidal level for experiment 1 and an increase in the tidal level for experiment 2. This was removed using a quadratic fit to characterize the uncertainty in water level. The detrended water level series had a standard deviation of 0.021 and 0.030 m for experiments 1 and 2, respectively. The autocorrelation function for the demean and detrended time series had a first zero crossing of 21 and 13 lags for experiments 1 and 2, respectively. Taking only every 21 and 13 observations as statistically independent, for experiments 1 and 2, the standard error of the mean was 0.006 and 0.009 m, respectively. Refer to **Table 4** for the statistics summary.

Table 4 Mean sea level (MSL) statistics at experiment locations

	Induced heave corrected			Induced heave uncorrected		
	MSL (m)	1-sigma	95%	MSL (m)	1-sigma	SEM
Experiment #1	–27.979	0.021	0.006	–27.979	0.021	0.006
Experiment #2	–26.759	0.030	0.009	–26.764	0.030	0.009

SEM: standard error of the mean.

Water level anomalies with respect to the NAD83 datum were estimated through the combinations of the filtered GNSS solutions and using the combined pressure and hydrographic data obtained at the pressure sensor location. The water level anomalies at the observation station were first compared to the corresponding water level anomalies from Dauphin Island's NOAA water level station. This was done to determine if reasonable water levels were estimated at the bottom pattern location. An estimation of a root mean square difference (rmsd) of 10 cm was obtained between the two anomalies. A conversion of the water level anomaly from the GNSS to a pressure anomaly resulted in a more accurate estimation, with an rmsd of 0.02 dbar (approximately 2 cm) compared to the pressure anomaly measured during the GNSS observation period. **Figure 9** shows that the water level peaks and troughs are aligned. Both water level anomalies captured three neap tides and two spring tides events. They also revealed the northern Gulf of Mexico sea level response to a tropical storm during a neap tide. Based on the correlation between the two water level anomalies, the ellipsoidally referenced water level from the pressure sensor will be used in the final tidal datums computations at the pressure sensor location.

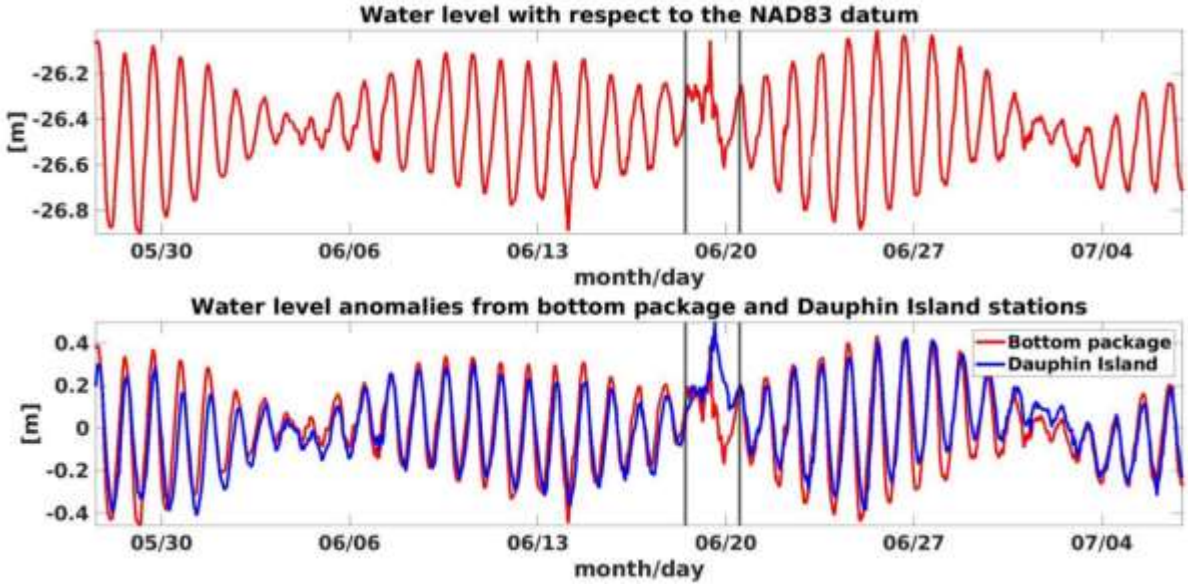

Figure 9 Top panel: water levels referenced to NAD83 datum. Bottom panel: water level anomalies from the bottom package and a nearby station.

5. DISCUSSION

Given that the results from the affordable and survey-grade hardware are very close (1-sigma = 5 cm), it is essential to emphasize that such positioning performance should not be misconstrued as rendering GNSS+INS sensors irrelevant in navigation applications. One may be tempted to reach that conclusion if one considers a unit vector whose origin is at the sensors, as we have shown here. Contrariwise, that would be far from true for much longer vectors where the effect of roll and pitch becomes apparent. A practical example is the case of single-beam and multi-beam SONARs for seafloor bathymetry relying solely on ray-tracing for sounding footprint localization on the seafloor, where the effects of roll and pitch can wrongly place a target some meters away from its correct locations, depending on the seafloor depth. Nevertheless, one can safely rely on GNSS-only PPP for positioning applications with very short antenna lever arms or vectors using a multi-frequency enabled affordable GNSS receiver in achieving vertical positioning accuracies better than 10 cm (95% ordered statistics) at an offshore location.

6. CONCLUSION

We describe a new water level measurement technique for tidal datum extension at offshore locations in addressing vandalization challenges with GNSS buoys. The technique utilized short-term PPP results from an affordable GNSS receiver aboard a USV and a pressure sensor deployed on the seafloor. As a first step toward the proof of concept, we evaluate the PPP results and show that 5-cm (1 sigma) uncertainty is possible with an affordable GNSS receiver, provided the PPP processing follows best practices and the GNSS-derived water levels apply a low-pass filter. Additionally, we show that a tilt sensor is unnecessary, provided the antenna lever arm is less than 0.5 m, confirming a submission from previous work. Accurate lever arm determination using precise instruments is also vital to overall accuracy. Finally, we present the preliminary water levels from the pressure sensor referenced to the ellipsoid. Future work will describe the computational procedure and analysis for the tidal datum extension in detail.

REFERENCES

Aggrey, J., Bisnath, S., Naciri, N., Shinghal, G., & Yang, S. (2019). Accuracy trend analysis of low-cost GNSS chips: The case of multi-constellation GNSS PPP. *Proceedings of the 32nd International Technical Meeting of the Satellite Division of the Institute of Navigation, ION GNSS+ 2019*, 3618–3635. https://doi.org/10.33012/2019.16971

André, B. G., Míguez, B. M., Ballu, V., Testut, L., & Wöppelmann, G. (2013). Measuring Sea Level with GPS-Equipped Buoys: A Multi-Instruments Experiment at Aix Island. *Measuring Sea Level with GPS-Equipped Buoys: A Multi-Instruments Experiment at Aix Island*, *10*(10), 27–38.

Arnell, J. T., Ingebrigtsen, I. F., Walb, S., & Roald, E. (n.d.). *A Comparison of Survey-Grade GNSS Receivers by Means of Observation and Coordinate Domain Approaches; Traditional Vs Low-Budget*. *September 2022*, 11–15.

Banville, S., Lachapelle, G., Ghoddousi-Fard, R., & Gratton, P. (2019). Automated processing of low-cost GNSS receiver data. *Proceedings of the 32nd International Technical*

Meeting of the Satellite Division of the Institute of Navigation, ION GNSS+ 2019, 3636–3652. https://doi.org/10.33012/2019.16972

Bisnath, S., Wells, D., Howden, S., & Stone, G. (2003). The use of a GPS-equipped buoy for water level determination. *Oceans 2003: Celebrating the Past... Teaming Toward the Future*, *3*(May 2014), 1241–1246. https://doi.org/10.1109/OCEANS.2003.178031

Cheng, K., Science, G., & Science, G. (2004). GPS Buoy Campaigns for Vertical Datum Improvement and Radar Altimeter Calibration. *Program*, *470*.

Dodd, D. (2009). Chart Datum Transfer Using a GPS Tide Gauge Buoy in Chesapeake Bay. *International Hydrographic Review*, *2*.

Gill, M., Bisnath, S., Aggrey, J., & Seepersad, G. (2018). Precise Point Positioning (PPP) using Low-Cost and Ultra-Low-Cost GNSS Receivers. *Proceedings of the 30th International Technical Meeting of The Satellite Division of the Institute of Navigation (ION GNSS+ 2017)*, *May*, 226–236. https://doi.org/10.33012/2017.15123

Gill, S. K., & Schultz, J. R. (2001). Tidal datums and their applications, NOAA Special Publication NOS-COPS 1. Retrieved on 1/15/2023 at https://www.tidesandcurrents.noaa.gov/publications/tidal_datums_and_their_applications.pdf.

Hare, R., Godin, A., & Mayer, L. (1995). *Accuracy Estimation of Canadian Swath and Sweep Sounding Systems*.

Hocker, B., & Wardwell, N. (2010). Tidal datum determination and VDatum evaluation with a GNSS buoy. *23rd International Technical Meeting of the Satellite Division of the Institute of Navigation 2010, ION GNSS 2010*, *3*, 2076–2086.

International Hydrographic Organization (IHO; 2020). International Hydrographic Organization Standards for Hydrographic Surveys, S-44 Edition 6.1.0. Retrieved on January 16, 2023, from https://iho.int/uploads/user/pubs/standards/s-44/S-44_Edition_6.1.0.pdf

Knight, P. J., Bird, C. O., Sinclair, A., & Plater, A. J. (2020). A low-cost GNSS buoy platform for measuring coastal sea levels. *Ocean Engineering*, *203*(February), 107198. https://doi.org/10.1016/j.oceaneng.2020.107198

Lin, Y. P., Huang, C. J., Chen, S. H., Doong, D. J., & Kao, C. C. (2017). Development of a GNSS buoy for monitoring water surface elevations in estuaries and coastal areas. *Sensors (Switzerland)*, *17*(1). https://doi.org/10.3390/s17010172

Lipatnikov, L. A., & Shevchuk, S. O. (2019). *Cost-effective precise positioning with GNSS* (Issue 74). https://www.fig.net/resources/publications/figpub/pub74/figpub74.asp

Nie, Z., Liu, F., & Gao, Y. (2020). Real-time precise point positioning with a low-cost dual-frequency GNSS device. *GPS Solutions*, *24*(1). https://doi.org/10.1007/s10291-019-0922-3

Nwankwo, U. C., Howden, S., & Wells, D. (2019). Further Investigations of VDatum to NAD83 Vertical Separations Using United States Geological Service (USGS) Coastal Water Levels Gage and Hydrolevel Buoy. *U.S. Hydrographic Conference*, *May* 1–12.

Nwankwo, Uchenna C., Howden, S., Wells, D., & Connon, B. (2020). Validation of VDatum in Southeastern Louisiana and Western Coastal Mississippi. https://doi.org/10.1080/01490419.2020.1846644, *44*(1), 1–25. https://doi.org/10.1080/01490419.2020.1846644

Oguntuase, J. O. (2020). Cost-Effective GNSS Hardware for High-Accuracy Surveys and Its Prospects for Post-Processed Kinematic (PPK) and Precise Point Positioning (PPP) Strategies. *Https://Aquila.Usm.Edu/Dissertations/1846*.

Parker, B., Milbert, D., Hess, K., & Gill, S. (2003). National VDatum - The Implementation of a National Vertical Datum Transformation Database. *Proceedings of the U.S. Hydrographic Conference*, *44*(9), 10–15.

Swanson, R. L. (1974). *Variability of tidal datums and accuracy in determining datums from short series of observations* (No. 64). National Ocean Survey.

Weston, D. N. D. and, & Dr. Volker Schwieger. (2010). *Cost Effective GNSS Positioning Techniques Cost Effective GNSS Positioning Techniques* (Issue 49).

BIOGRAPHICAL NOTES

Johnson Oguntuase is an Assistant Professor of Hydrographic Science at the University of Southern Mississippi (USM), where he brings his expertise to life in the classroom with his teachings in Kinematic Positioning, Applied Acoustics, and Applied Bathymetry. With a Ph.D. in Marine Science (Hydrographic Science) and an MSc. in Geodesy, his recent endeavors show his passion for the field. He is dedicated to developing cost-effective processing strategies for high-accuracy positioning at sea using affordable GNSS receivers and tactical-grade INS. Before his academic career at USM, Dr. Oguntuase was a licensed surveyor and a successful business owner in Nigeria, where he offered services to engineering consulting companies and government agencies. He is a member of the Hydrographic Society of America (THSOA) and a professional member of the Institute of Navigation (ION).

CONTACTS

Johnson Oguntuase
University of Southern Mississippi
1020 Balch Blvd
Stennis Space Center, MS
USA
+1 228-688-3389
Johnson.oguntuase@usm.edu

Uchenna Nwankwo
Texas A&M Geochemical and Environmental Research Group (GERG)
833 Graham Road,
College Station TX 77845
USA
Uchenna.nwankwo@tamu.edu

Stephan Howden
University of Southern Mississippi
1020 Balch Blvd
Stennis Space Center, MS
USA
1-228-688-5284
Stephan.howden@usm.edu